Numerical simulation of distortion and phase transformation in laser welding process using MSC Marc/Mentat

D Sebayang[1], YHP Manurung[2], A Ariri[1], O Yahya[2], H Wahyudi[1], AK Sari[1], and D Romahadi[1]

[1] Faculty of Mechanical Engineering, Mercu Buana University, Jakarta Indonesia
[2] Advanced Manufacturing Technology Excellence Center (AMTeX), Faculty of Mechanical Engineering Universiti Teknologi MARA (UiTM), Shah Alam Malaysia

E-mail: darwin.sebayang@mercubuana.ac.id

Abstract. In this paper, numerical simulation of distortion and phase transformation in laser welding process is carried out. *A* coupled thermal-structural and metallurgical model of laser welding process is simulated by using FEA engineering software MSC Marc/Mentat. The specimen model is simulated in the form of butt joint plate with dimension 50 mm in length and 25 mm in width with 2 mm thickness and using material low carbon steel (C15). Conical heat source model implemented in this simulation due to existing Goldak's double ellipsoid commonly used for arc welding process. Phase transformation is predicted based on Seyyfarth-Kassatkin Model and implemented in user subroutine PLOTV which is written in FORTRAN programming language. Presented results of laser welding simulation included temperature distribution, phase transformation, and estimated welding distortion.

Keywords: finite element method, simulation, distortion, phase transformation, t8/5, laser welding

1. Introduction

The development of technology encourages the development of various welding techniques such as by joining material using laser technology. Many ways are done to obtain good properties of laser welding joints. Experimental research are conducted to know the phenomena in laser welding process but it is expensive and time-consuming [1-3]. Nowadays, welding simulation is conducted to predict the output of welding process which will help to reduce the cost in term of experimental research. It was common in industrial manufacturing especially in the automobile industry.

When conducting welding simulation in FEM. Heat source model should be important factor to be considered. Mostly, goldak double ellipsoid model used in simulation of an arc welding process. However, in the other welding process such as laser welding, the Goldak model could not represent actual heat source model accurately [4]. The conical heat source model is developed in order to simulated laser welding process accurately. Conical heat source model implemented by add user defined subroutine in MSC marc/mentat software. Unlike the cylindrical model, the conical model takes into account the varying intensity of the heat flux, whereby the intensity of the heat flux is higher at the centre of the cone and also decreases in intensity with the depth [5]. The microstructure formation have big impact in determining the residual stress in welding process. [6].

IOP Conf. Series: Materials Science and Engineering **453** (2018) 012020 doi:10.1088/1757-899X/453/1/012020

Numerical analysis of laser welding with consideration of phase transformations and mechanical properties of welded joints were presented. The analytical models concern to predicting of the phase transformation in the heat-affected zone (HAZ) based on chemical composition by using Seyffarth-Kassatkin (1984) model. Seyffarth-Kassatkin model depends on the time it takes for cooling the material from 800 to 500 ^{O}C and known as the t8/5. Cooling time widely used in welding industry to control phase changes during welding process. Other researcher also use $T_{8/5}$ for determining phase transformation [7].

2. 3D finite element model

Three dimensional model of specimen simulated with dimension of each plate is 50 mm length, 25 mm length and 2 mm thickness. Figure 1 illustrated schematic drawing of the specimen competed with quad meshing and table. Four point load applied to illustrated clamping condition.

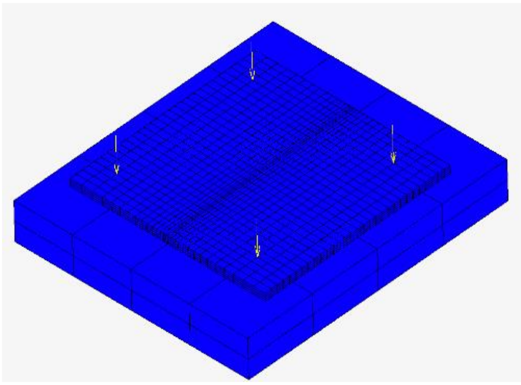

Figure 1. Model specimen in MSC Marc/mentat

In this simulation, C15 steel is chosen as a material plate due to closeness in term of material properties of mild steel. Physical properties and chemical composition of material are shown in table 1 and table 2 below.

Table 1. Material properties of C15 steel

Welding parameter	Value
Young's Modulus (GPa), E	210
Minimum yield strength, γ (MPa)	300
Poisson's ratio, ν	0.3
Density, ρ (kg/m³)	7850
Melting temperature, t_m (°C)	1540

Table 2. Chemical properties of C15 steel (%)

Steel	C	Si	Mn	Al	Cu	Cr	Ni	Mo	Ti
C15	0.15	0.22	0.41	0.0005	0.15	0.06	0.06	0.036	0.0

In this study, the conical heat source model based on the work of Zhan et al. is used [5, 8-9]. However several researcher is also improved and developed conical heat source [10-12]. The conical heat source is represented by the equation below.

$$Q_v = \frac{9Q_0}{\pi(1-e^{-3})} \cdot \frac{1}{(z_e-z_i)(r_e^2+r_e r_i+r_i^2)} \cdot \exp\left(-\frac{3r^2}{r_c^2}\right) \quad (1)$$

$$Q_0 = \eta P \quad (2)$$

$$r_c = f(z) = r_i + (r_e - r_i)\frac{(z-z_i)}{(z_e-z_i)} \quad (3)$$

Qv represents the net heat flux and Q_0 represents the product of laser beam energy in (P) in watts and η the efficiency value. Rc represent the heat distribution coefficient as a function of z direction. r(e) represent the maximum radius of the cone and ri represent the minimum radius of the cone. Figure 2 below illustrates the conical heat source model.

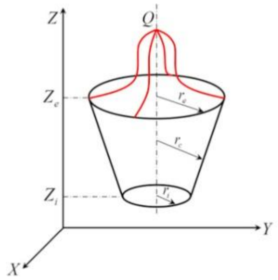

Figure 2. Conical heat source model

Heat source parameter used in this simulation summarize in table 3 below.

Table 3 Heat Source Dimension in FEM Simulation

Heat Source Direction	Value
Power, Q (watt)	700
Max radius, r_e (mm)	1
Min radius, r_i (mm)	0.5
Depth, z_i (mm)	2
Welding travel speed, v (mm/s)	7

The ambient temperature of the environment is defined to be at 30° Celsius. Heat loss due to contact with the table is also considered by applying a contact heat transfer coefficient of 1000 W/m^{2}K while the film coefficient is defined at 25 W/m^{2}K.

Phase transformation calculation is done by using Seyffarth-Kassatkin model which is hugely depend on cooling temperature time $T_{8/5}$ [13].. The volume fraction of particular phase transformation such as martensite, perlite, bainite, and ferrite describe in the equation below:

$$ln\, t_M = 2.1 + 15.5C + 0.84Si + 0.96Mn + 4.0Al + 0.8Cu + 0.77Cr + 0.7Ni + 0.74Mo + 0.3V + 0.5W - 13.5C^2 \quad (4)$$

$$ln\, T_M = 0.56 - 0.41C + 0.1Mn + 0.5Cu + 0.14Cr - 0.3Mo + 2.7Ti + 1.1Nb + 1.7C * Mo \quad (5)$$

$$ln\, t_{FP} = 0.34 + 5{,}2C + 0.53Si + 1.8Mn + 1.0Cu + 0.33Cr + 1.3Ni + 2.9Mo + 1.5W - 5.1C^2 \quad (6)$$

$$ln\, T_{FP} = 0.91 - 0.9C + 0.09Mn + 0.08Cr + 0.15Ni + 0.34Mo + 0.85V + 2.2Ti + 0.43W \quad (7)$$

$$\ln t_F = 0.66 + 10.0C - 0.48Si + 1.3Mn + 1.3Cr + 1.2Ni + 1.5Mo - 1.4W + 3.5C * Mn - 5.9C^2 \quad (8)$$

$$\ln T_F = 1.23 - 0.37Si + 0.17Mn - 0.3Cu + 0.3Cr + 0.31Ni - 0.5Mo + 0.09Nb - 0.43W \quad (9)$$

t is the starting time of formation for each phase, and T, represents the end time. M for martensite, FP for ferrite-pearlite, and F for ferrite. C, Si, Mn, Cu, Cr, Ni, Mo, and W is represents the percentage of each element in the material composition of the workpiece. while tA in the equation represents the t8/5. the percentage of ferrite, pearlite, bainite and martensite are calculated by the following equations [14].

$$F_{max} = 100 * \left(1 - \frac{C - 0.02}{0.81 - 0.11Mn - 0.05Mo}\right) \quad (10)$$

$$M = 100 * \left[1 - \Phi\left(\frac{\ln t_{85} - \ln t_M}{\ln T_M}\right)\right] \quad (11)$$

$$FP = 100 * \Phi\left(\frac{\ln t_{85} - \ln t_{FP}}{\ln T_{FP}}\right) \quad (12)$$

$$F = F_{max} * \Phi\left(\frac{\ln t_{85} - \ln t_F}{\ln T_F}\right) \quad (13)$$

$$P = FP - F \quad (14)$$

$$B = 100 - M - FP \quad (15)$$

$$\Phi(x) = \frac{1}{\sqrt{2\pi}} \int_{-\infty}^{x} e^{-\frac{1}{2}x^2} * dt \quad (16)$$

M, represents the percentage distribution of Martensite, F, represent the percentage of Ferrite-Perlite, F represent the percentage of Ferrite, P represent the percentage of Pearlite and B represent for the percentage of Bainite. The percentage of each phase is calculated using the cumulative distribution function (ϕ) with the starting and ending time of formation.

3. Result and discussion

Laser welding simulation with conical heat source model using subroutine UWELDFLUX in MSC Marc/Mentat has been conducted successfully.

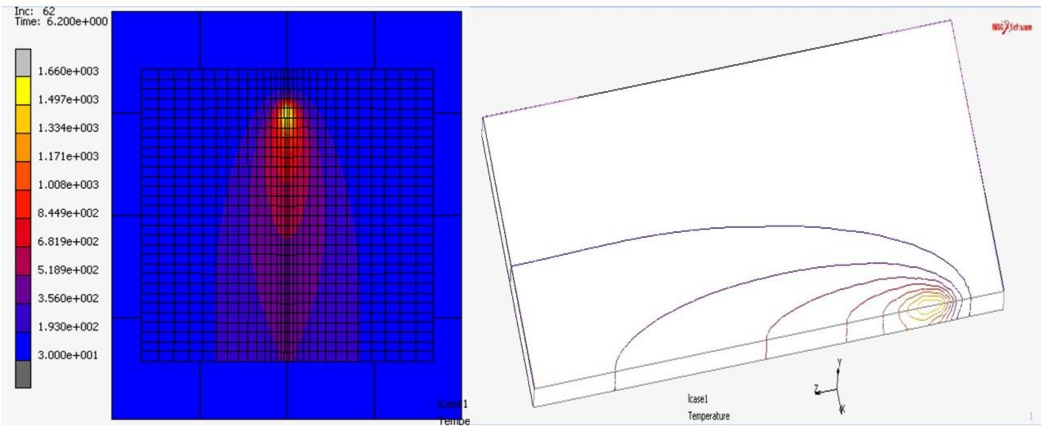

Figure 3. Numerically estimated temperature of laser welding process

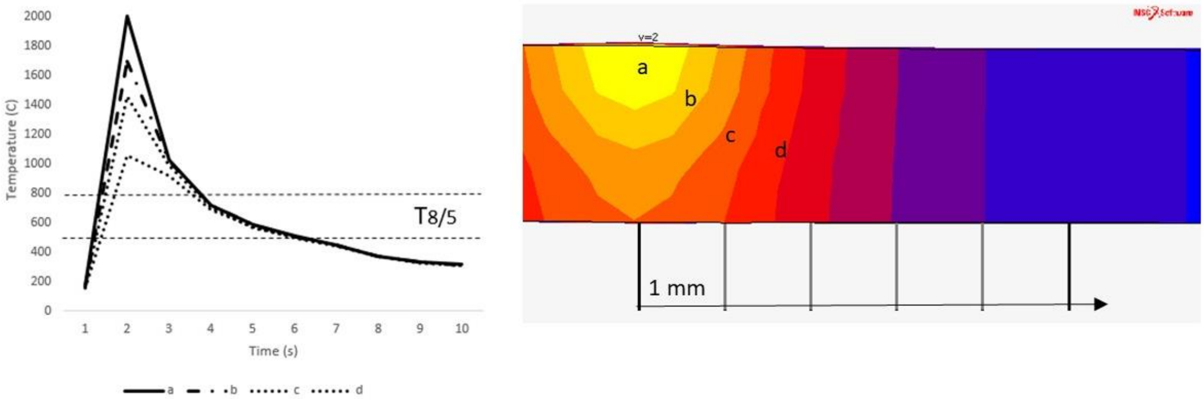

Figure 4. Temperature distribution in different length of HAZ

Temperature distribution of laser welding process presented in figure 3. Cooling time ($T_{8/5}$) as a basic factor to determine phase transformation also can be seen in figure 4. However, $T_{8/5}$ has been calculated successfully by implementing user subroutine PLOTV for predicting phase transformation.

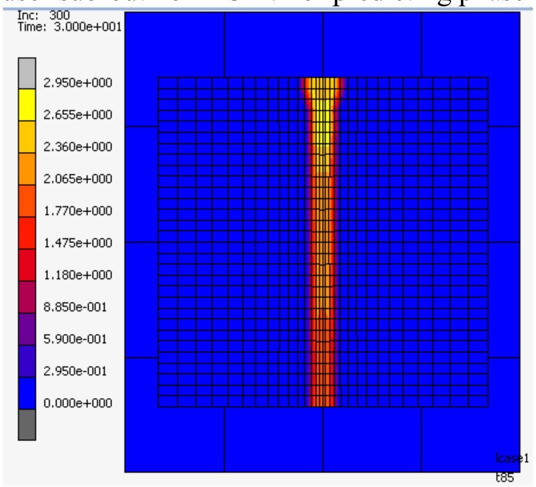

Figure 5. predicted $T_{8/5}$

Figure 5 shows the time taken for the node to cooling down from temperature 800 to 500 ^{O}C. Maximum value of $T_{8/5}$ observed around 3 second. In the start of welding path, show that cooling down time is faster compare to the end of weld path. It is because in the start of welding simulation surrounding area is defined into ambient temperature which makes the plate are relatively cool. Distribution of phase transformation fraction showed in figure 6 below.

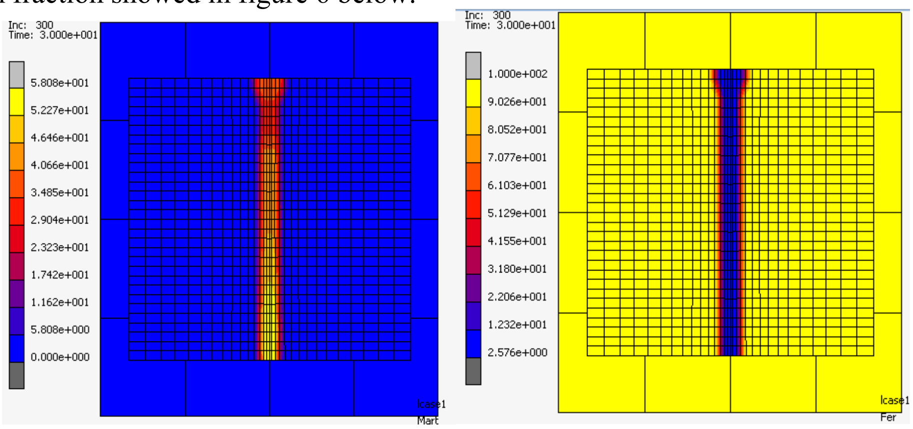

Martensite Ferrite

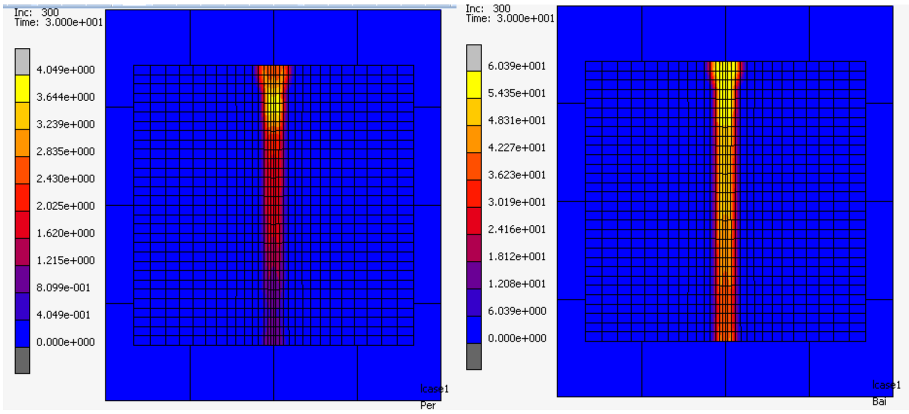

Perlite Bainite

Figure 6. Predicted phase transformation

The simulation result of phase transformation show the structural composition of butt welding consist of martensite, bainite, perlite and minor ferrite. It also show correlatively between cooling time $T_{8/5}$ and martensite formation since the major martensite formation occurring in the rapid cooling area. However, the accuracy in this simulation is approximate at best. Since the model in this simulation is mild steel with many chemical composition. However, the specimen model only takes several chemical composition elements, usage of other elements which is not define in the specimen model may cause inaccuracy.

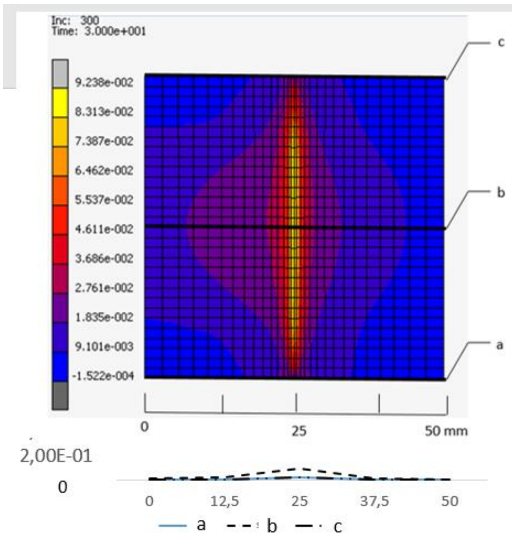

Figure 7. Distribution of displacement along *y* axis

The predicted distortion in welding process presented in figure 7. It can be shown that distortion along y axis is relatively small and reaches the peak in the heat source zone. However, representation of clamping (shown in figure 1), give significant benefit to reduce welding distortion.

4. Conclusion

Numerical simulation of laser welding has been conducted successfully. Representation of clamping in the simulation also decreased displacement at the output of welding process. Phase transformation using Seyffarth-Kassatkin model by developing user subroutine PLOTV shows good result. Major Martensite formation occur in the start of welding path due to rapid cooling and minor ferrite in the heat affected zone. However, by using finer mesh and greater number of increment it can be greatly improve accuracy of the simulation, but it will consuming more calculation time. Hence, meshing should be considered wisely.

Simulation of welding process is very important not only to reduce defect of welded, but also to achieve good and expected mechanical properties. Further investigation of phase transformation and the effect of mechanical properties would give beneficial for the future studies.

5. Acknowledgement

The authors would like to express their gratitude to the faculty of mechanical engineering Mercubuana University and Advanced Manufacturing Technology Excellence Centre (AMTEx) at Faculty of Mechanical Engineering, Universiti Teknologi MARA (UiTM) Malaysia for encouraging this investigation.

References

[1] Steen W M, 1990 *Laser Material Processing* London; Springer
[2] Piekarska W, Kubiak M, and Saternus Z, 2012 *Archives of Metallurgy and Materials*. **4** 1219
[3] Piekarska W, Saternus Z, Kubiak M, and Domański T 2015 *METAL 2015 Proceedings*. 736
[4] Wu C, Hu Q and Gao J, 2009 *Computational Materials Science,* **46(1)** 167
[5] Omar Y, Yupiter H P M, Mohammad S S, Keval P P, Abdul R O, Wahyu K, Henning V W, Alexandwe B, and Marcel G 2017 Virtual Manufacturing for Prediction of Martensite Formation and Hardness Value induced by Laser Welding Process using Subroutine Algorithm in MSC Marc/Mentat**,** *ICAME Proceeding*.
[6] Xavier C, Delgado J, Castro, J. and Ferreira, A, 2017 Numerical Predictions for the Thermal History, Microstructure and Hardness Distributions at the HAZ during Welding of Low Alloy Steels
[7] Piekarska W, Goszczynska D, and Saternus Z, 2015 *Journal of Applied Mathematics and Computational Mechanics*, **14(2)** 61
[8] Zhan X, Liu Y, Ou W, Gu C and Wei Y, 2015 *Journal Of Materials Engineering And Performance,* **24(12)** 4948
[9] Zhan X, Li Y, Ou W, Yu F, Chen J, and Wei Y, 2016 *Optics & Laser Technology,* **85** 75
[10] Sun J, Liu X, Tong Y and Deng D 2014 *Materials & Design,* **63** 519
[11] Shanmugam N, Buvanashekaran G, and Sankaranarayanasamy K, 2009 *Experimental Techniques*, **34(5)** 25
[12] Mwema F, 2017 *International Journal of Nonferrous Metallurgy*, **06(01)** 1
[13] Seyffarth P, Kasatkin O G, 1979 *Mathematisch-statistische Beschreibung der Austenitumwandlung in der Wärmeeinflußzone, Schweißtechnik,* **29** 117
[14] Seyffahrt P, Kassatkin O G, 1984 *Rechnerische Bestimmung der prozentualen Gefügezusammensetzung in der Wärmeeinflußzone niedriglegierter Stähle*